Preferred citation: T. Wahlström. Predictions of MD and CD tensile property profiles. In **Advances in Pulp and Paper Research, Cambridge 2013**, *Trans. of the XVth Fund. Res. Symp. Cambridge, 2013*, (S.J. I'Anson, ed.), pp 673–710, FRC, Manchester, 2018. DOI: 10.15376/frc.2013.2.673.

PREDICTIONS OF MD AND CD TENSILE PROPERTY PROFILES

*Torbjörn Wahlström**

ABSTRACT

To design new and optimize existing paper and board material an understanding of how the paper making process affects the final paper properties and how we can control them is neccesary. There is a link missing between pulp properties and machine made paper properties. The aim with this work is to close this gap by proposing an engineering model which, based on furnish properties, makes it possible to predict tensile property profiles in MD and CD.

Two series of hand sheet trials were made to validate and formulate the model. The purpose with the first trial was to validate that the geometric mean of the studied properties in MD and CD is constant and equal to the isotropic value. The second trial was made to find relations between anisotropies of the studied properties and the fibre anisotropy.

The model was applied on a press draw trial made on a production machine. The strain and tensile property profiles were measured and predicted based on laboratory measurements on the furnish. The predictive capability of the model was regarded as fairly good, especially since the general behaviour of the paper properties was correctly captured. The deviation of predictions compared to measurements were around 10% or less for most of the evaluated positions and properties, except for MD tensile energy absorption index that was poorly predicted.

* Corresponding address: Torbjörn Wahlström (torbjorn.wahlstrom@storaenso.com) Stora Enso AB, Box 9090, 650 09 Karlstad, Sweden, +46 737 090165.

Keywords: Simulation, model, paper, board, pulp, furnish, shrinkage, stretch, strain, drying, isotropic, anisotropic, anisotropy, paper properties, tensile stiffness, tensile index, strain at break, tensile energy absorption, TEA, Profile, CD profile, MD draw, Wet draw, Web tension

INTRODUCTION

To design new and optimize existing paper and board material we need to understand how the paper making process affects the final paper properties and how we can control them. There is a link missing between furnish properties and machine made paper properties. The aim with this work is to close this gap by proposing an engineering model which, based on furnish properties, makes it possible to predict tensile property profiles in MD and CD.

Shrinkage and stretch of wet paper will have a great effect on most of the paper properties and is used as a starting point for this work. There are linear relations between in plane tensile properties and total strain accumulated during drying for isotropic handsheets (Wahlström and Fellers 2000). The linear behaviour is valid also for anisotropic paper as shown by Wahlström and Fellers (1999) and Mäkelä (2003, 2009).

Next step is to be able to predict anisotropic behaviour based on isotropic properties as measured on hand sheets. A useful quantity for comparing paper with different fibre anisotropies is the geometric mean of MD and CD properties. Schrier and Verseput (1967) found that the geometric mean or square root of MD times CD taber stiffness was independent of, or invariant to, changes in fibre anisotropy. Later de Ruvo et al (1976) showed that the geometric mean coincided with the properties of an isotropic handsheet made of the same raw material. Htun and Fellers (1982) found, for a few mechanical properties, that the geometric mean value of MD and CD properties is constant and equal to the isotropic quantity, but restricted to a given shrinkage and stretch combination in MD and CD. Wahlström (2004) showed that the geometric mean of MD and CD free drying strain also is independent of changes in fibre orientation anisotropy. Wahlström (2009) gave the geometric mean a theoretical background by showing that it is equal to the mean value of the property distribution in the plane of the paper. Wahlström and Mäkelä (2005) proposed a method to predict anisotropic behaviour for tensile stiffness and shrinkage based on isotropic input. The method combined the earlier mentioned invariance of the geometric mean of MD and CD properties and relations between anisotropies for restrained and free dried properties as well as fibre anisotropy.

Regarding prediction of MD and CD property profiles Constantino et al (2005) proposed and demonstrated a model for the CD shrinkage profile. The model explained differences in shape caused by differences of furnish, machine design and operating conditions during experiments on two paper machines. Wahlström et al (1999) used an orthotropic constitutive model for plane stress to predict the stresses and strains that develop in a paper web during its transportation through a cylinder drying section. CD tensile stiffness and shrinkage profiles were predicted and the latter compared to a real case. Mäkelä (2003) also used numerical analysis of the mechanics of the paper web during its passage through the drying section and laboratory experiments to predict tensile stiffness profiles in MD and CD. Wahlström (2012) used the model proposed by Constantino et al (2005) to predict the contraction profile resulting from a machine trial with varying press draw. Results from the same trial has been used for prediction of tensile property profiles in this work.

The model proposed in this work accounts for fibre orientation, press draw, shrinkage potential of the furnish and dryer geometries which are all important factors affecting the tensile properties of paper and board. The engineering prediction aspect of the work is of great priority. Constitutive modelling and finite element methods are great tools but not so easy to use for an average engineer. The purpose is to propose a readily available and intuitively understandable model, without compromises on the results. Two series of hand sheet trials are made to validate and formulate the model. The purpose with the first trial was to validate that the geometric mean of the studied properties in MD and CD is constant and equal to the isotropic value. The second trial was made to find relations between anisotropies of the studied properties and the fibre anisotropy. The model is applied on a press draw trial made on a production machine making bleached kraft paper. The strain and tensile property profiles in MD and CD were measured and predicted based on laboratory measurements on the furnish.

MATERIALS AND METHODS

Hand sheet trials – Constant geometric mean and relations between anisotropies

Purpose. The hand sheet trials were made for two reasons. First to validate the assumption that the geometric mean of the studied properties in MD and CD is constant and equal to the isotropic value (Equation 6 to Equation 8). Second to validate the proposed relations between anisotropies of the studied properties and fibre anisotropy (Equation 12 to Equation 20).

Machine Chest Furnishes. Furnish was taken from the machine chests for the middle and bottom ply of a board mill. The middle ply furnish (22,5 ºSR) contained CTMP, low yield sulphate, broke and a small amount highly refined sulphate. The bottom ply furnish (25,0 ºSR) was an unbleached low yield sulphate. Anisotropic handsheets were made in a Formette dynamic sheet former with a conditioned basis weight of 110 g/m^2 for restrained dried sheets. The speed of the drum was 1100 rpm and a nozzle pressure of either 2,0; 2,5 or 3,0 bars were used to produce paper sheets with different fibre anisotropy. The handsheets were couched using only two blotters to keep the sheets wet. Pressing was made in a static press with 400 kPa during 5 minutes. Either of two different drying strategies regarding external boundary conditions was adopted, restrained or free drying. In the results middle ply is represented by closed circles and bottom ply by open circles.

The restrained dried handsheets were dried in an STFI plate dryer. In the plate dryer, described by Htun and Fellers (1982), the sheet is clamped between two rigid and heated drying frames. The mean density for the restrained dried sheets was 347 kg/m^3 for the middle ply furnish and 530 kg/m^3 for the bottom ply furnish. The freely dried handsheets were dried between two steel wires separated by a distance large enough to avoid external forces restricting the shrinkage, but small enough to avoid large scale buckling of the paper. Drying time was 25 minutes in an oven at 105 ºC and thereafter conditioned over night in 50% RH and 23 ºC. The free drying strain was determined by measuring the distance between two marks in the paper before drying and after conditioning. The method is described in closer detail by Wahlström and Goldszer (2004). Material testing was made after conditioning.

Single Pulp Furnishes. A CTMP pulp (freeness 411 CSF) and a softwood bleached sulphate pulp (24,0 ºSR) were taken from a board mill. Formette sheets were made with the speed of the drum set to 1100 rpm and the nozzle pressure to 2,0; 2,5 and 3,0 bars for each pulp. The conditioned basis weight was 80 g/m^2. Pressing was made in a roll press, first pressing at 250 kPa and secondly at 450 kPa. The samples were dried restrained in an STFI plate dryer. In the results CTMP is represented by closed squares and sulphate by open squares. Data for tensile stiffness and free drying strain has earlier been published from this trial by Wahlström (2005).

Once Dried Furnishes. Bales of bleached sulphate pulp and rolls of recycled liner were slushed and anisotropic handsheets with three different degrees of anisotropy were made with a Formette handsheet former. The target grammage for the sulphate handsheets were 50 gsm and for the liner handsheets 110 gsm. Pressing of the anisotropic handsheets were made at 300 kPa to achieve similar density as for the isotropic handsheets. The handsheets were dried with two different drying strategies regarding external boundary conditions, restrained and free. In the results sulphate is represented by closed diamonds and liner by open diamonds. Data for tensile stiffness and free shrinkage strain has earlier been published from this trial by Wahlström (2004).

Testing Methods. The fibre anisotropy was evaluated by Stora Enso Karlstad Research Centre using an image analysing method. A transparent adhesive tape was applied to both sides of the sample and then the tapes were pulled apart, leaving a layer of fibres on each of the two tapes. A new tape was applied to the delaminated surface and the tapes were pulled apart again etc. The samples in this study were separated into about 25 layers. A reflectance image against black background was produced on each layer using a scanner. The images were subsequently analysed to determine the fibre segment angle distribution of each layer. Thereafter a von Mises distribution function was fitted to the experimental data. The analysis and parameter definitions are described in detail by Rigdahl and Hollmark (1986). The number of fibre segments oriented in MD divided by the number of fibre segments oriented in CD was defined as the fibre anisotropy (short for fibre segment angle distribution anisotropy). The average of the evaluated fibre anisotropy of each layer was used as the fibre anisotropy of the sample. The thickness of the samples was measured with an L&W micrometer according to EN 20534 and tensile properties according to SCAN P 67:93.

Machine trial

To test the proposed model a trial with varying press draw was made on a production machine making bleached kraft paper. The 70 g/m^2 kraft paper was formed on two Fourdriniers, pressed in a Combi press, a single felted roll Press (diameter 1,1 m) and dried in a conventional double felted Drying section with a free draw length of 1,965 m. The differential speed (jet– wire) was 5,0 m/min in both top and bottom layer. Press loads were 71 kN/m in the Combi press and 90 kN/m in the 2nd press. The solids content after press was around 36 % (moisture ratio 1,8 kg/kg). The calender was not used during the trial.

The press draw was first reduced as much as possible throughout the press section. This resulted in a 2,3 % stretch between the Combi press and the 2nd press and 0,7 % between the 2nd press and first dryer group (Figure 1). The web width, W, at the reel (measured off line on a CD reel sample) was 5,36 m. Thereafter the machine speed of the first dryer group of 584 m/min was increased in steps up to 597 m/min, or a further 2,2 % stretch whereafter a web break occurred. The MD draw or stretch was measured with a tachometer directly on the cylinders and was found to agree with the control system. The free draw length, L^P, after the 2nd press was between 550 mm and 1100 mm, these are the distances to the first lead roll (A) and the drying section fabric guide roll (B) respectively. With a width-to-length ratio well above one, an uneven contraction across the web width can certainly be expected.

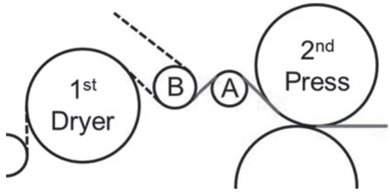

Figure 1. Press draw between 2nd press and 1st dryer group in a kraft paper machine.

The shrinkage profiles were measured at UMIST by detecting variations in the pitch of the forming fabric marks in the paper caused by shrinkage (I'Anson et al 2008). A trimmed web width of 5,537 m going into the press section was taken from the computer system and used for analysis.

Restrained and free dried isotropic handsheets made from the furnish used in the machine trial were used as input to the predictions. The handsheets were pressed with three different pressures to create a relation between tensile properties, free drying strain and density. Interpolation was used to find the tensile properties and free drying strain at the same density as the paper produced in the machine trial. In the results below only the properties at the correct density are reported.

The model proposed below was applied for the machine trial to predict MD and CD tensile property profiles based on handsheet measurements and machine parameters as input.

MODEL FOR PREDICTIONS

Total Strain Accumulated during Drying

An extension or contraction of a wet paper will have a great effect on most of its paper properties and is used as the starting point for the model described here. Relative elongation or strain, ε (%), according to Equation 1, is used to characterize the deformation where δ (m) is the elongation and L (m) the original length of a sample.

$$\varepsilon = \frac{\delta}{L} \tag{1}$$

In papermaking the deformation can be either mechanical due to application of external forces, hygroscopic due to a change of the water content in the paper or a combination thereof. Both can induce either extension or contraction of the paper although a mechanical extension and hygroscopic contraction is the prevailing mechanisms. The mechanical extension, often called wet stretch or draw, is referred to as mechanical strain, ε^m. The contraction of the paper due to a reduction of the water content through drying is often called shrinkage, but is here referred to as hygroscopic strain, ε^h. The total strain, ε, that accumulates in a paper during the papermaking process is the sum of the hygroscopic and mechanical strain according to Equation 2. A negative total strain is often referred to as shrinkage, a positive as stretch and a zero total strain after drying as restrained drying (*r*). A standard so called hand sheet is dried restrained, meaning that no hygroscopic strain is allowed to develop and no mechanical strain is induced in the paper, leading to zero total strain. With no external forces applied to the paper during drying the hygroscopic strain will reach its maximum referred to as free drying (*f*). An illustration of different types of strain induced in the paper during papermaking is given in Figure 2.

$$\varepsilon = \varepsilon^h + \varepsilon^m \tag{2}$$

When a positive mechanical strain is applied (stretch) in one in-plane direction of the paper it will lead to negative strain (contraction) in its transverse direction. The strain in the transverse direction, ε_2, can be predicted from the applied strain,ε_1, with Equation 3. v (dimensionless) is the Poisson ratio for which a value of 0,293 can be used for isotropic paper (Baum et al 1981). Figure 3 shows CD contraction as a result of MD straining of a narrow strip of paper. An isotropic paper is a paper with the same properties in all in-plane directions.

$$\varepsilon_2^m = -v \cdot \varepsilon_1^m \tag{3}$$

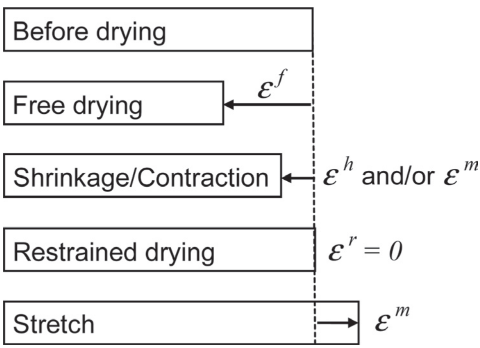

Figure 2. Illustration of different types of strain induced in paper during papermaking.

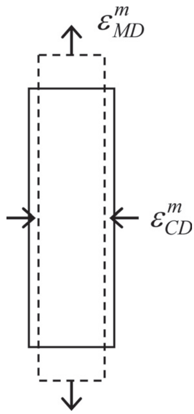

Figure 3. Contraction in CD due to a stretch in MD.

Relations between Tensile Paper Properties and Total Strain

As referred to in the introduction there are linear relations between in plane tensile properties and total strain accumulated during drying. This means measurements on two papers made with different total strain accumulated during drying are needed to predict the properties for any total strain. For experimental reasons it is suitable to choose restrained and free drying. Restrained drying corresponds experimentally to standard hand sheet procedures giving zero percent total strain after drying (ε^r). So called free drying, drying without any external forces acting on the paper, results in maximum shrinkage, here referred to as free drying strain (ε^f). Free drying strain can be measured for example according to Wahlström and Goldszer (2004). Thickness of free dried handsheets are allways higher compared to restrained dried. How much of the thickness increase that can be attributed to a structural change in the bulk of the paper compared to only the surface is not clear. In the proposed model the density is assumed to be constant with varying total strain. With knowledge of the free drying strain and the tensile properties for a free and a restrained dried isotropic handsheet tensile stiffness index, tensile index, strain at break and tensile energy absorption can be calculated for any total strain using Equation 4. Figure 4 shows predicted tensile stiffness index, E (MNm/kg), tensile index, σ_T (kNm/kg), strain at break, ε_T (%) and tensile energy absorption or TEA index, W (J/kg) using Equation 4. The predictions are based on the furnish data from the machine trial in this work where isotropic hand sheets were dried restrained and free. The data has been normalised based on the restrained dried property to be able to compare the sensitivity of the different properties to free drying strain. Input data used is given in Table 1.

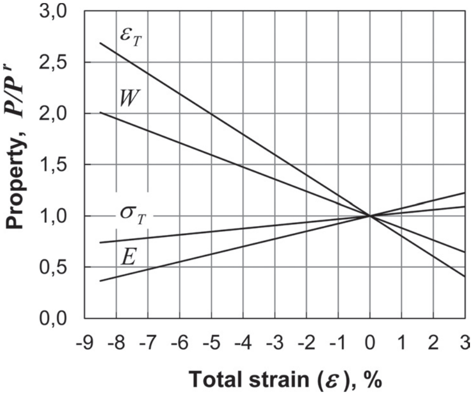

Figure 4. Predicted relations between in-plane isotropic tensile properties and total strain accumulated during drying normalised with the restrained dried value.

$$P = \frac{P^r - P^f}{\varepsilon^r - \varepsilon^f}\varepsilon + P^r \quad \left(P = E,\ \sigma_T,\ \varepsilon_T,\ W\right) \tag{4}$$

Fibre Anisotropy

How the fibres are orientated in a paper is principally controlled by effects in the headbox contraction and when the jet impinges on the wire. The accelerating flow causes the fibres to orient in the direction of the flow since the different ends of the fibres are subjected to different flow velocities. This effect is at a minimum when the jet and wire velocities are the same and becomes more significant as the velocity differential increases in either direction. The degree of fibre orientation can be characterized by the anisotropy of the paper. An anisotropy is often defined as the ratio of some property in the two principal in-plane directions of paper, the machine or manufacturing direction, MD, and the cross machine direction, CD. Equation 5 defines the fibre orientation anisotropy, $A(F)$ (dimensionless), hereafter referred to as fibre anisotropy, where n is the relative number of fibres in the respective in-plane direction.

$$A(F) = \frac{n_{MD}}{n_{CD}} \tag{5}$$

A useful quantity for comparing paper with different fibre anisotropies is the geometric mean of MD and CD properties. It is assumed that the isotropic values of the properties discussed in this work are equal to the geometric mean of the MD and CD value according to Equation 6 to Equation 8. Results showing this for all tensile properties dealt with in this work have not previously been published and therefore the behaviour is validated in the experimental results from this study in *Figure 13* to *Figure 21*.

$$P^r_{Iso} = \sqrt{P^r_{MD} \cdot P^r_{CD}} \quad \left(P = E,\ \sigma_T,\ \varepsilon_T,\ W\right) \tag{6}$$

$$P^f_{Iso} = \sqrt{P^f_{MD} \cdot P^f_{CD}} \quad \left(P = E,\ \sigma_T,\ \varepsilon_T,\ W\right) \tag{7}$$

$$\varepsilon^f_{Iso} = -\sqrt{\varepsilon^f_{MD} \cdot \varepsilon^f_{CD}} \tag{8}$$

In Equation 9 to Equation 11 anisotropies for the properties in Equation 6 to Equation 8 are defined to be able to calculate anisotropic properties based on the isotropic properties and fibre anisotropy.

$$A(P^r) = \frac{P^r_{MD}}{P^r_{CD}} \quad \left(P = E,\ \sigma_T,\ \varepsilon_T,\ W\right) \tag{9}$$

$$A(P^f) = \frac{P^f_{MD}}{P^f_{CD}} \quad \left(P = E,\ \sigma_T,\ \varepsilon_T,\ W\right) \tag{10}$$

$$A(\varepsilon^f) = \frac{\varepsilon^f_{MD}}{\varepsilon^f_{CD}} \tag{11}$$

Equation 12 to Equation 20 are empirically derived to describe the relations between the anisotropies defined in Equation 9 to Equation 11 and fibre anisotropy, $A(F)$. Wahlström and Mäkelä (2005) previously showed the validity of Equation 12, Equation 13 and Equation 20. The relations for tensile index, strain at break and tensile energy absorption index, Equation 14 to Equation 19, is based on the results from this work (*Figure 22* to *Figure 30*).

$$A(E^r) = A(F) \tag{12}$$

$$A(E^f) = 2A(F) - 1 \tag{13}$$

$$A(\sigma^r_T) = A(F) \tag{14}$$

$$A(\sigma^f_T) = 1{,}33A(F) - 0{,}33 \tag{15}$$

$$A(\varepsilon^r_T) = 1 \tag{16}$$

$$A(\varepsilon^f_T) = 1/\left(0{,}25A(F) + 0{,}75\right) \tag{17}$$

$$A(W^r) = A(F) \tag{18}$$

$$A(W^f) = 0{,}25A(F) + 0{,}75 \tag{19}$$

$$A(\varepsilon^f) = 1/A(F) \tag{20}$$

From Equation 6 to Equation 20 it is possible to calculate the tensile properties and free drying strain in MD and CD both for free and restrained drying based on the isotropic properties and fibre anisotropy. *Figure 5* and *Figure 6* shows the effect of an increasing fibre anisotropy on tensile stiffness index, E, tensile index, σ_T, strain at break, ε_T, tensile energy absorption index, W, and free drying strain, ε^f, in MD and CD for restrained and free drying respectively. All properties are normalised with its respective isotropic value.

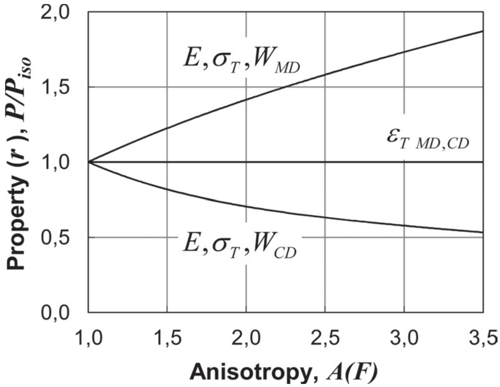

Figure 5. Predicted normalised tensile properties in MD and CD for restrained drying as a function of fibre anisotropy.

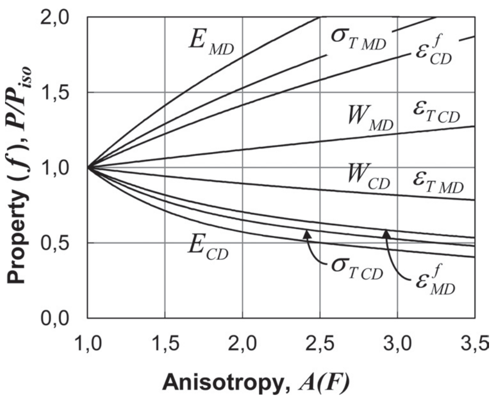

Figure 6. Predicted normalised tensile properties in MD and CD for free drying as a function of fibre anisotropy.

Equation 4 described isotropic behaviour. Since Wahlström and Fellers (1999) as well as Mäkelä (2003) has showed linear relations, between total strain accumulated during drying and tensile properties, also for anisotropic paper Equation 4 can be extended to Equation 21 and Equation 22. Equation 27 to Equation 42 in Appendix 1 gives tensile stiffness index, tensile index, strain at break, tensile energy absorption and free drying strain in the MD and CD direction and for free and restrained drying as a function of the respective isotropic property and fibre anisotropy. This means that Equation 21 and Equation 22 together with Equation 27 to Equation 44 makes it possible to predict anisotropic properties for an arbitrary total strain accumulated during drying and fibre anisotropy based on isotropic handsheet data. *Figure 7* to *Figure 10* shows examples where tensile stiffness index, tensile index, strain at break and tensile energy absorption index, ε^f has been predicted based on the same isotropic hand sheet data from the machine trial earlier used for the predictions in Figure 4.

$$P_{MD} = \frac{P^r_{MD} - P^f_{MD}}{\varepsilon^r_{MD} - \varepsilon^f_{MD}} \varepsilon_{MD} + P^r_{MD} \quad \left(P = E,\ \sigma_T,\ \varepsilon_T,\ W\right) \tag{21}$$

$$P_{CD} = \frac{P^r_{CD} - P^f_{CD}}{\varepsilon^r_{CD} - \varepsilon^f_{CD}} \varepsilon_{CD} + P^r_{CD} \quad \left(P = E,\ \sigma_T,\ \varepsilon_T,\ W\right) \tag{22}$$

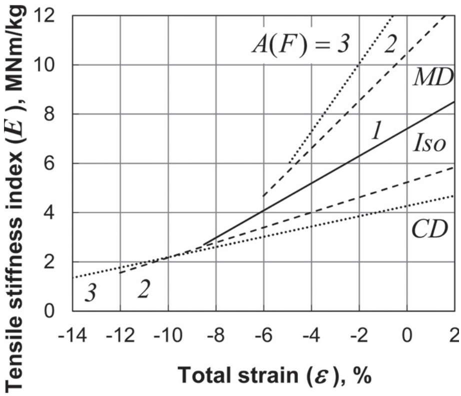

Figure 7. Prediction of tensile stiffness index in MD and CD for different fibre anisotropies and total strain based on isotropic data.

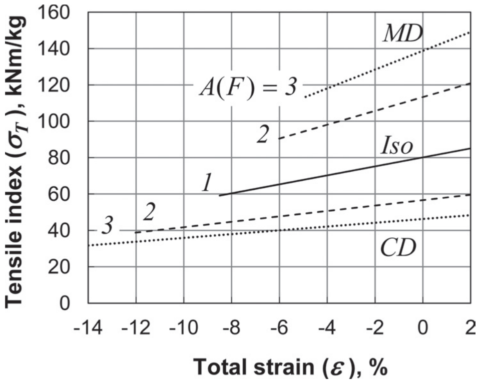

Figure 8. Prediction of tensile index in MD and CD for different fibre anisotropies and total strain based on isotropic data.

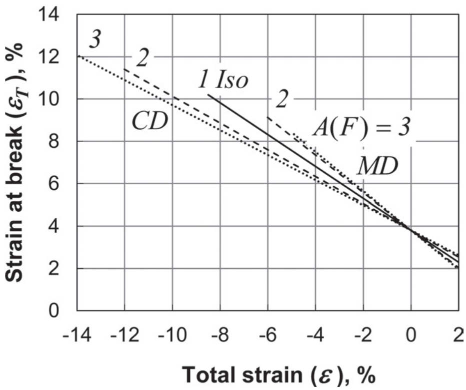

Figure 9. Prediction of strain at break in MD and CD for different fibre anisotropies and total strain based on isotropic data.

Press Draw Contraction

Between press nips and between last press and first dryer group the speed of the web is increased to maintain the runnability. The relative speed increase is normally named press draw and given as a percentage. Typically a press draw between last press and first dryer group can be in the order of 2–3 %. This MD draw or strain will result in a CD contraction as described in Equation 3 for a narrow strip of paper. In a press draw in a paper machine the paper web that is

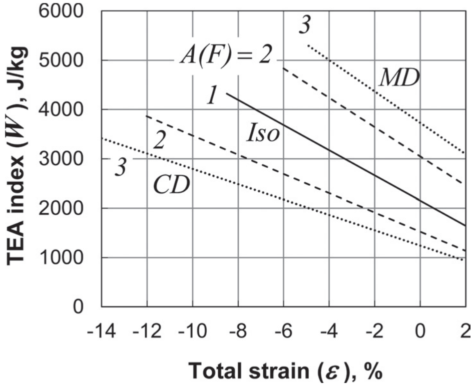

Figure 10. Prediction of TEA index in MD and CD for different fibre anisotropies and total strain based on isotropic data.

stretched is wide in CD and short in MD. In such a geometry we have to consider the boundary conditions since the CD contraction will not be evenly distributed in CD. At the very edge of the web the loading condition will be uniaxial and in the middle biaxial as illustrated in Figure 11.

The contraction in CD, ε_{CD}^{m}, which is a result of mechanical stretch in MD, can be calculated according to Equation 3 for a narrow strip of paper. Equation 3 however assumes elastic behaviour and suggests a linear relation between CD contraction and MD strain. Recently Wahlström (2012) showed a strong non elastic behaviour for paper stretched in a wet state according to Equation 23. With increasing MD strain (ε_{MD}^{m}) the CD strain for a narrow strip of paper decreases exponentially. The fitting parameter *a* is dependent of the moisture ratio of the paper. The second fitting parameter *b* is constant for varying moisture ratio and defines the generic shape of the relation.

$$\varepsilon_{CD}^{m} = ae^{b\varepsilon_{MD}^{m}} - a \tag{23}$$

Constantino et al (2005) suggested that CD shrinkage at a point in a paper after drying in a cylinder drying section depends on the distance of that point from both edges of the sheet and on the length of the unsupported draws in the dryer section. With this assumption it was possible to successfully predict the results by Wahlström and Lif (2003) who made laboratory measurements of shrinkage along the centre line between two jaws holding paper samples during drying. Their results also confirmed the importance of the shape of the free draw. Thus it was demonstrated that the width and length, whether varied separately or combined, controlled

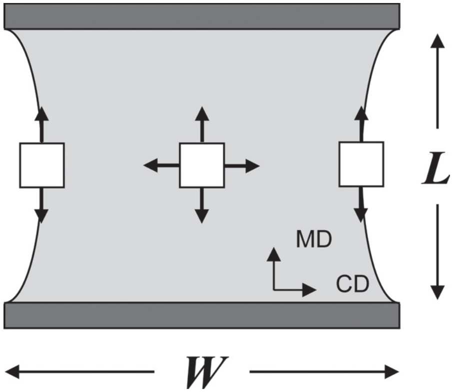

Figure 11. Uniaxial and biaxial stress in a free draw.

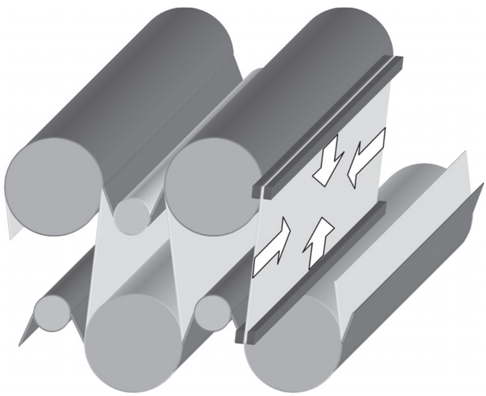

Figure 12. A multi cylinder dryer section.

the resulting shrinkage profile. Due to the free edge in a free draw the contraction at the edge should be free and unchanged. To adapt the model to this behavior a third correction term was added that made the edge value equal to the CD contraction as a result of an MD strain. In Equation 24 $\varepsilon^p_{CD}(x)$ (%) is the strain in CD at the CD position x as a result of the MD strain or press (p) draw. ε^m_{MD}. W^p (m) is the width of the web, L^p (m) the length of the press draw and K^p a constant.

$$\varepsilon^p_{CD}(x) = \varepsilon^m_{CD}\left(e^{-\frac{K^p x}{L^p}} + e^{-\frac{K^p (W^p - x)}{L^p}} - e^{-\frac{K^p W^p}{L^p}} \right) \tag{24}$$

Drying Shrinkage

It is well known that the CD shrinkage is higher at the edges of a paper web compared to the middle. The reason for this is the geometries and the prevailing boundary conditions in the free draws of the dryer section of the paper machine. Figure 12 shows a double felted multi cylinder drying section. The free draw is the area where the web is not restrained by the drying fabric. As illustrated in the figure two of the edges in the free draw are fixed by the fabric and two edges are free. Figure 11 shows the resulting stress states from the border conditions in the free draw. In the middle part of the web the paper is under biaxial stress and at the very edge under uniaxial stress. The uniaxial stress state at the edge means that the CD shrinkage is made as free drying, there are no external forces restricting the shrinkage. The CD shrinkage at the very edge can be assumed to be equal to the free drying strain of the paper, ε^f_{CD}. The distribution of the drying strain in CD, $\varepsilon^d_{CD}(x)$, along the width, x (m), can then be calculated with Equation 25. $M\varepsilon^f_{CD}$ (%) is the free drying strain or shrinkage potential in CD, W^d (m) is the width of the web, L^d (m) is the length of the free draw and K^d is a tuning parameter that may depend on the number of free draws in the drying section. Finally however the drying, and thereby also the shrinkage, does not only take place in the free draws but also in a restrained state under the drying fabric. The relative amount of drying in the free draw is accounted for by the tuning parameter F^d which is a fraction of one, in this case 0,62, meaning that the free drying strain is reduced by 38%.

$$\varepsilon^d_{CD}(x) = F^d \cdot \varepsilon^f_{CD}\left(e^{-\frac{K^d x}{L^d}} + e^{-\frac{K^d (W^d - x)}{L^d}} - e^{-\frac{K^d W^d}{L^d}} \right) \tag{25}$$

CD total strain profile

The total strain controls the paper properties. The profile in total strain is the sum of the press draw contraction profile and the drying shrinkage profile. Equation 26 is valid for each position x along the width of the web.

$$\varepsilon_{CD} = \varepsilon^p_{CD} + \varepsilon^d_{CD} \tag{26}$$

RESULTS

Hand sheet trials

Constant geometric mean. The results from the handsheet trials are here used to validate an assumption that the geometric mean of the MD and CD value is constant and equal to the isotropic value for the studied in-plane tensile properties at restrained and free drying strain (Equation 6 to Equation 8). *Figure 13* and *Figure 14* shows the geometric mean of the tensile stiffness index in MD and CD for restrained and free dried handsheets respectively. The geometric mean has been normalized with the isotropic value to show the deviation clearly. As the isotropic value the mean of the geometric means for different fibre anisotropies was used. *Figure 15* to *Figure 21* also shows the geometric mean for restrained and free dried handsheets with varying fibre anisotropy but for tensile index, strain at break, tensile energy absorption index and free drying strain. In general the geometric mean was constant with varying fibre anisotropy for all studied cases. The deviation was around +/– 10%.

In *Figure 13* to *Figure 21* the circles represents the results from the trial with machine chest furnishes, open circles are from sheets made with bottom ply

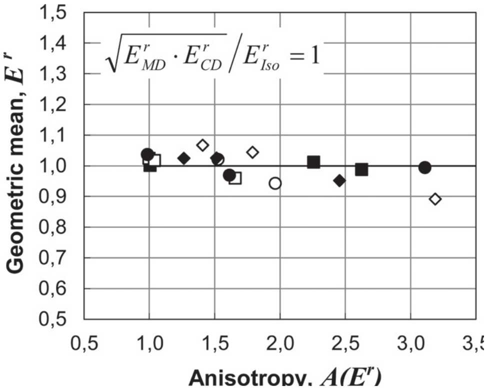

Figure 13. Normalised geometric mean of restrained dried tensile stiffness index in MD and CD versus anisotropy.

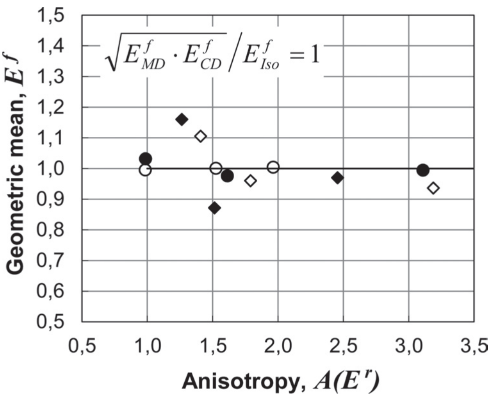

Figure 14. Normalised geometric mean of free dried tensile stiffness index in MD and CD versus anisotropy.

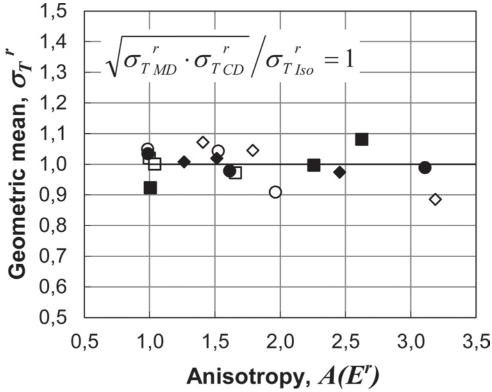

Figure 15. Normalised geometric mean of restrained dried tensile index in MD and CD versus anisotropy.

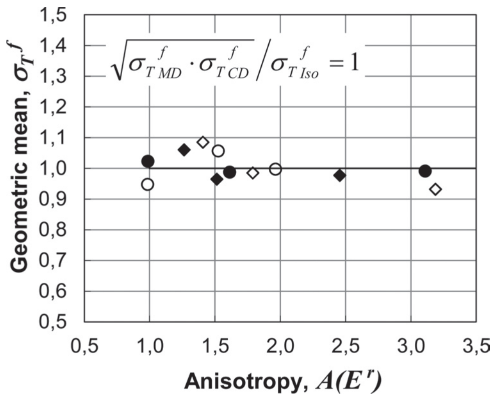

Figure 16. Normalised geometric mean of free dried tensile index in MD and CD versus anisotropy.

furnish and closed middle ply furnish. Open squares represents bleached sulphate and closed squares CTMP sheets from the trial with single pulp furnishes. Finally from the trial with once dried furnishes the open diamonds represents recycled liner and closed diamonds bleached sulphate bale pulp.

Relations between anisotropies. The results from the handsheet trials evaluated as anisotropies are the base for Equation 12 to Equation 20 which describe the relations between the anisotropies defined in Equation 9 to Equation 11 and fibre anisotropy, $A(F)$. *Figure 22* shows a 1:1 relation between tensile stiffness index

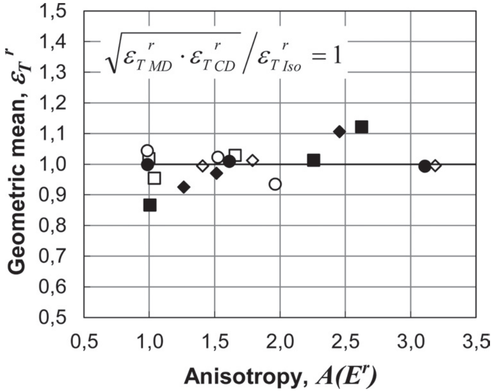

Figure 17. Normalised geometric mean of restrained dried strain at break in MD and CD versus anisotropy.

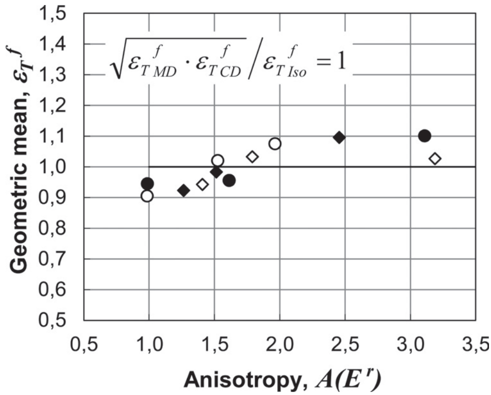

Figure 18. Normalised geometric mean of free dried strain at break in MD and CD versus anisotropy.

anisotropy and fibre anisotropy for restrained dried papers. For free dried papers the relation between tensile stiffness index anisotropy for free dried paper and restrained dried papers had a larger slope (*Figure 23*). *Figure 24* to *Figure 30* also shows the relations between the different anisotropies described above but for tensile index, strain at break, tensile energy absorption index and free drying strain. The different marker types have the same meaning as in *Figure 13* to *Figure 21*. The relations for tensile index was similar to the relations for tensile stiffness index

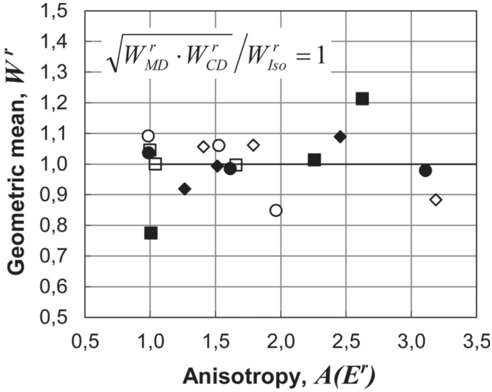

Figure 19. Normalised geometric mean of restrained dried TEA index in MD and CD versus anisotropy.

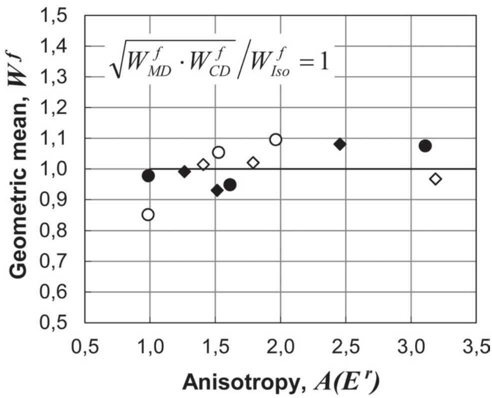

Figure 20. Normalised geometric mean of free dried TEA index in MD and CD versus anisotropy.

but the slope for free dried papers versus restrained dried is smaller. For strain at break the relation was constant and equal to one at restrained drying and for free drying it decreased exponentially. Also the free drying strain relation decreased exponentially. The TEA anisotropy showed a 1:1 relation for restrained drying and a weak increase for free drying.

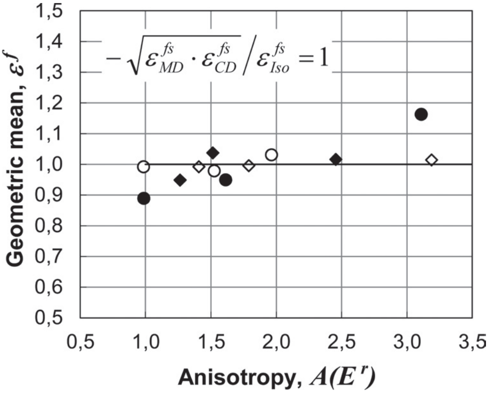

Figure 21. Normalised geometric mean of free drying strain in MD and CD versus anisotropy.

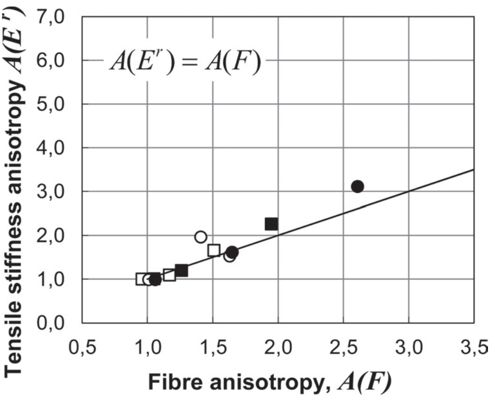

Figure 22. Tensile stiffness index anisotropy versus fibre anisotropy for restrained dried papers.

Machine trial

To test and demonstrate the proposed model the results from a machine trial with varying press draw was evaluated and predicted. In a reference case the press draw was reduced as much as possible and thereafter, in the "Increased draw" case, the draw was increased in steps until a web break occured. Tensile properties measured on restrained and free dried isotropic handsheets were used as input

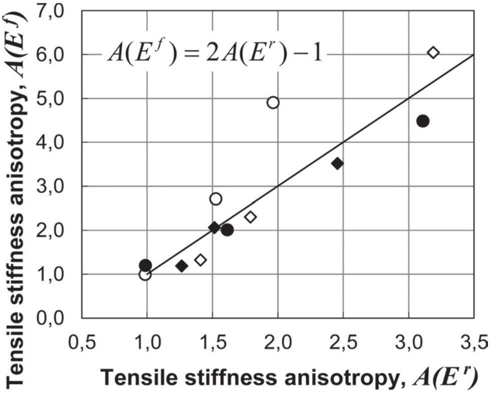

Figure 23. Tensile stiffness index anisotropy for free dried paper versus restrained dried papers.

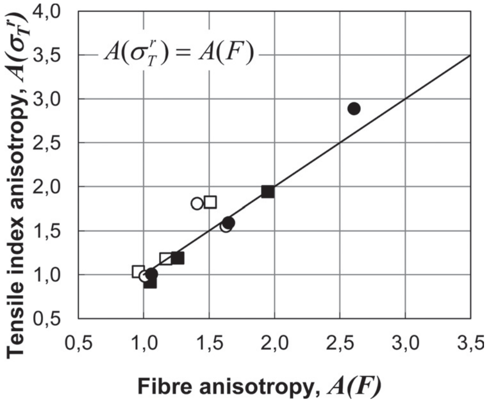

Figure 24. Tensile index anisotropy versus fibre anisotropy for restrained dried papers.

parameters to the predictions (Table 1). Handsheets were made from the same furnish that was run during the machine trial. The resulting properties were interpolated to the same density, 685 kg/m^3, as for the paper produced during the machine trial.

Table 2 shows the input parameters to the model measured on the paper or paper machine. As the fibre orientation anisotropy the tensile index anisotropy

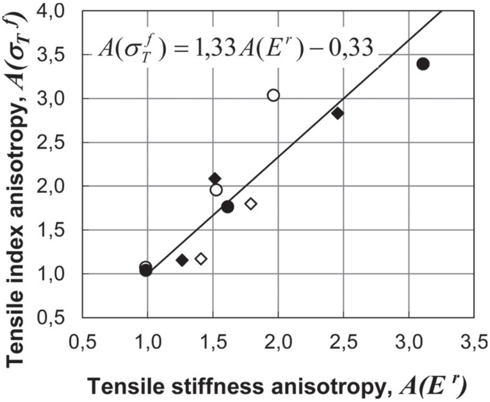

Figure 25. Tensile index anisotropy for free dried paper versus tensile stiffness anisotropy for restrained dried papers.

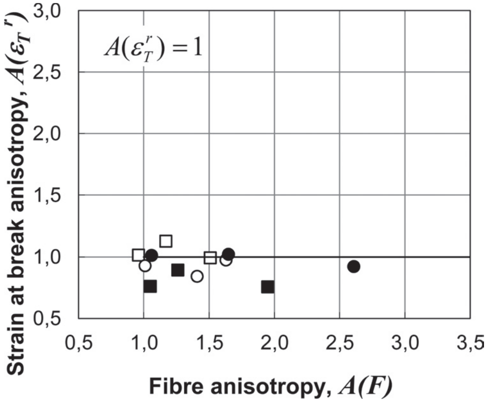

Figure 26. Strain at break anisotropy versus fibre anisotropy for restrained dried papers.

Table 1. Input parameters, measured on handsheets

	Restrained	*Free*
Tensile stiffness index (E), MNm/kg	7,4	2,7
Tensile index (σ_T), kNm/kg	80,1	59,2
Strain at break (ε_T), %	3,8	10,2
Tensile energy absorption index (W), J/kg	2153	4320
Free drying strain (ε^f), %		–8,5

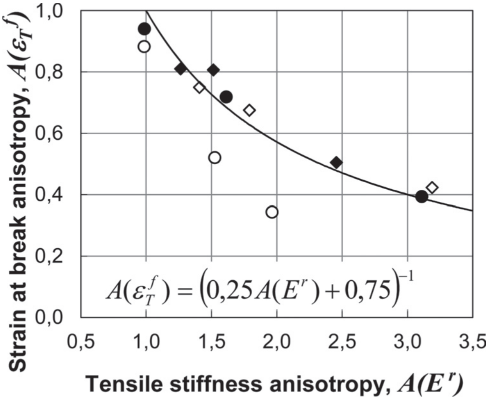

Figure 27. Strain at break anisotropy for free dried paper versus tensile stiffness anisotropy for restrained dried papers.

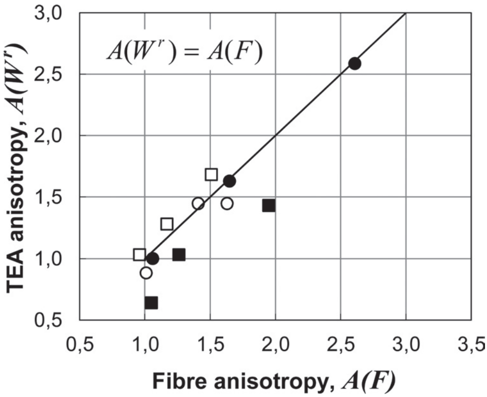

Figure 28. TEA index anisotropy versus fibre anisotropy for restrained dried papers.

Table 2. Input parameters (variables), measured on paper and machine

	Reference	*Increased draw*
Fibre orientation anisotropy ($A(F)$, –	1,24	
Web width (W^p and W^d), m	5,36	
Press draw length (L^p), m	0,8	
Dryer free draw length (L^d), m	1,95	
MD strain (ε^m_{MD}), %	0,7	2,9

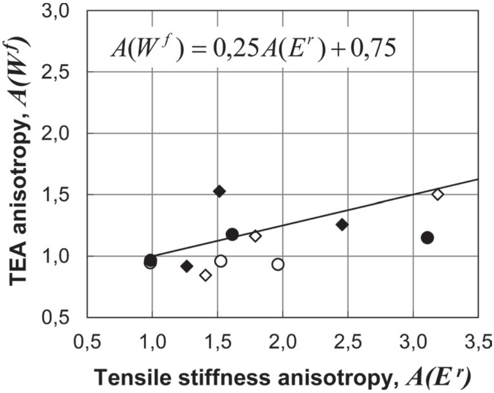

Figure 29. TEA index anisotropy for free dried paper versus tensile stiffness anisotropy for restrained dried papers.

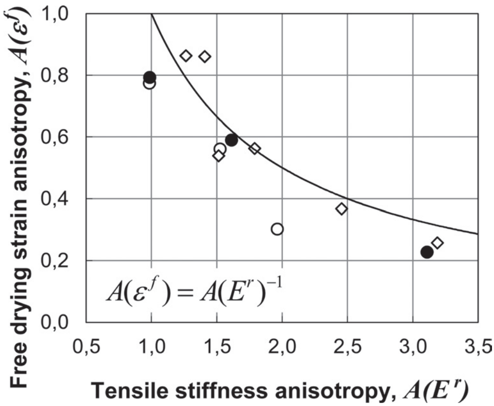

Figure 30. Free drying strain anisotropy versus tensile stiffness anisotropy for restrained dried papers.

(MD/CD) was used, the MD and CD value respectively was the average of the values from the full web width. The same web width, measured on the reel for the reference case, was used in both the reference case and in the case with increased press draw. The free length of paper between second press and dryer section is named press draw length and was measured during the trial. The length of the free

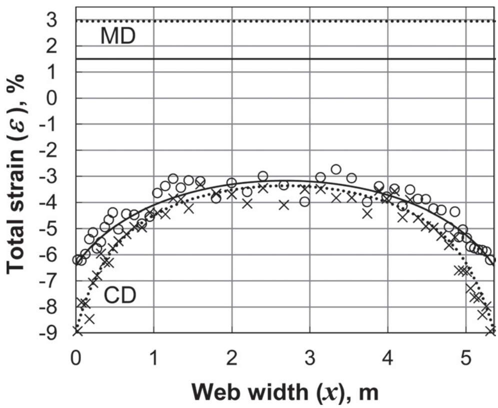

Figure 31. Measured and predicted total strain versus web width position for the reference case (circles, solid line) and increased draw case (crosses, dotted line).

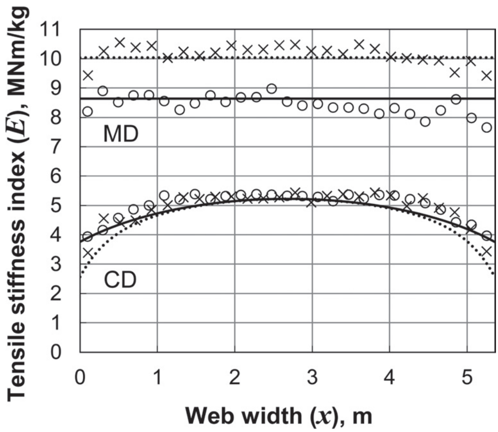

Figure 32. Measured and predicted tensile stiffness index in MD and CD versus web width position for the reference case (circles, solid line) and increased draw case (crosses, dotted line).

draw in the dryer section was measured on a drawing of the dryer section. The MD strain or press draw was measured with a tachometer during the machine trial.

Starting with the reference case the first step in making the predictions was to tune the edge value of CD strain to the measured edge value by adjusting the

Table 3. Input parameters, fixed and for tuning

	Both cases	*Type*
Relative free drying (F^d), –	0,62	Tuning
Dryer free draw (K^d), –	0,9	Tuning
CD contraction (a), –	–0,5	Tuning
CD contraction (b), –	0,66	Fixed
Contraction profile (K^p), –	2,3	Fixed

"Relative free drying" parameter (F^d). Thereafter the mid web CD strain was adjusted using the "Dryer free draw" parameter" (K^d). The CD contraction parameter (a), was used to adjust the contraction in CD, ($\varepsilon^m{}_{CD}$), to measured data. The CD contraction parameter b was a fixed value defining a general shape of the exponential relation according to Wahlström (2012). A fixed value was also used for the "Contraction profile parameter" K^p earlier used by Wahlström (2012). When predicting the case with increased draw only the MD draw was changed, from 0,7% to 2,9%.

Figure 31 shows CD strain, as measured by analysis of wire markings, versus web width position. Circles represents the reference case and crosses the case with increased draw. The increased draw contributed to the CD strain profile as a larger contraction (reduced strain) at the edges compared to the middle. Also the predicted result is shown in the figure, where the solid lines represents the reference case and the dotted lines the increased draw case. The agreement in CD is good but the model was also tuned after these experimental results. MD strain was not evaluated experimentally and the lines indicating predictions are for this case rather to be seen as an illustration of input data, representing the 0,7 and 2,9 % MD strain.

Figure 32 shows measured and predicted tensile stiffness index in MD and CD versus web width position for both the reference and increased draw case. The markers and line types have the same meaning as in Figure 31. As for the total strain profile the results show that MD draw contributed to CD tensile stiffness index profile with a reduction at the edges. Figure 33 to Figure 35 shows the same type of results as Figure 32 but for tensile index, strain at break and tensile energy absorption index. As expected from the hand sheet trials the results for tensile index showed low sensitivity to shrinkage, Figure 33. Figure 34 shows a strong influence from shrinkage for strain at break with increasing edge values for increased draw. MD strain at break decreased with increased MD draw. For the increased draw case the agreement was good. Tensile energy absorption index, Figure 35, showed a general behaviour similar to strain

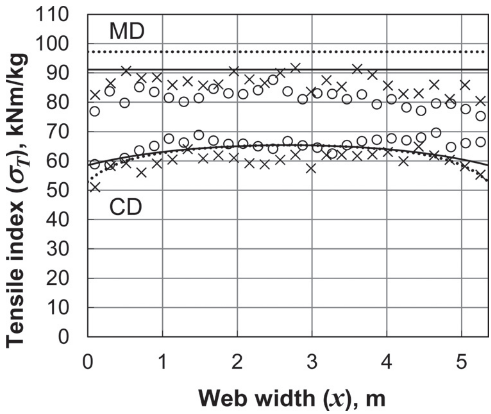

Figure 33. Measured and predicted tensile index in MD and CD versus web width position for the reference case (circles, solid line) and increased draw case (crosses, dotted line).

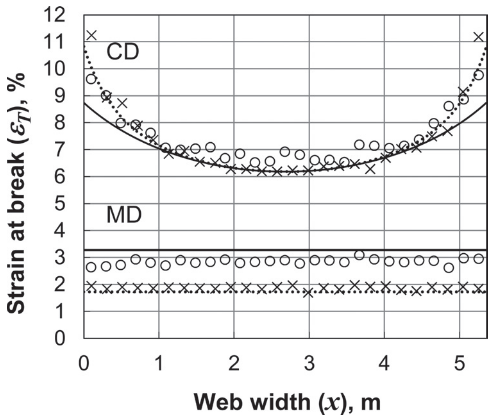

Figure 34. Measured and predicted strain at break in MD and CD versus web width position for the reference case (circles, solid line) and increased draw case (crosses, dotted line).

at break with higher values in CD, compared to MD, and higher values at CD edges.

The deviation of predictions from measurements, as shown in Figure 32 to Figure 35, are given in Table 4. For the MD profile the deviation was evaluated as an average of all web width positions. For the CD profile the middle (mid)

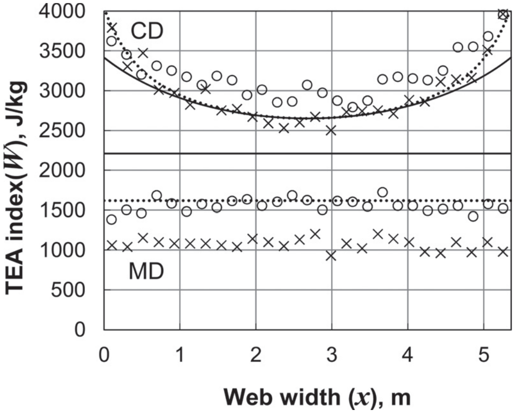

Figure 35. Measured and predicted tensile energy absorption index in MD and CD versus web width position for the reference case (circles, solid line) and increased draw case (crosses, dotted line).

Table 4. Deviation of predictions from measurements in Figure 32 to Figure 35.

Tensile property	*Reference case*			*Increased draw case*		
	MD	*CD mid*	*CD edge*	*MD*	*CD mid*	*CD edge*
Tensile stiffness index	3 %	–2 %	–1 %	–1 %	–2 %	11 %
Tensile index	12 %	0 %	–5 %	12 %	8 %	8 %
Strain at break	16 %	–9 %	–12 %	–7 %	–2 %	–11 %
TEA index	42 %	–10 %	–12 %	51 %	–1 %	0 %

was defined as the average of all values between 2 and 4 meters web width. The CD edge value is the average of the two edge values at the points where the measurements were made.

DISCUSSION

The relations between anisotropies as evaluated in the handsheet trials were central for the proposed model predicting anisotropic behavior at varying total strain. Even though the experimental results originated from six different furnishes it should be emphasized that Equation 12 to Equation 20 were empirically derived to describe the relations between the anisotropies defined in Equation 9 to Equation 11. More experimental work should be made to evaluate possible differences between furnishes and also the influence from the experimental methods used. A possibility to establish a physical base for the proposed relations could be to study their behavior through net-work modeling. Meanwhile some speculation can be of interest as a start to understand the underlying mechanisms. Consider a schematic fibre network with increasing fibre anisotropy, A, and fibres of equal properties according to *Figure 36*. For the isotropic case ($A = 1$) there are seven fibres in MD and CD meaning that the average number of fibres for all in-plane directions is also seven, however only MD and CD is shown. The geometric mean, $\sqrt{MD \cdot CD}$, of number of fibres in MD and CD is constant with increasing fibre anisotropy (Wahlström 2009). Given this the number of fibres in MD and CD are given for $A = 2$ and 3 according to Figure 36. Starting with restrained drying it is reasonable to assume a 1:1 relation between tensile stiffness and fibre anisotropy according to *Figure 22* if each fiber can carry one "unit" of load for a small extension. A 1:1 relation is also valid for the data produced by Setterholm and Kuenzi (1970) and Hasuike et al (1987). The same reasoning as for tensile stiffness can be applied on tensile strength (*Figure 24*) but for load at break as directly proportional to the number of fibres. Strain at break however has the anisotropy one or is the same in MD and CD at restrained drying (Htun and Fellers 1982, Wahlström et al 2000). This also shows in *Figure 26* and means that the stretch of the paper before it breaks does not change with the number of fibres in a certain direction. It is the fiber type, bonding, treatment and other factors that influence how much the fibres can be stretched before breakage or pulled out from the fibre network that governs the level of strain at break. The tensile energy absorption is the area under the stress strain curve and therefore dependent of the previously mentioned three properties. The experimental result in *Figure 28* shows a 1:1 relationship to fibre anisotropy.

At free drying the shrinkage takes place mainly at the bonding sites of a fibre network (Nanko and Wu 1995). Based on this the development of the free drying strain can be understood with reference to *Figure 36*. Assume that each fibre crossing leads to one unit of free drying strain in MD and CD. The free drying anisotropy (Equation 11) is then 7/7, 5/10 and 4/12 for a fibre anisotropy of 1, 2 and 3 which fits Equation 20 with reference to the experimental results in Figure 30. The anisotropy in tensile stiffness is larger for a certain fibre anisotropy at free drying compared to restrained drying (Equation 12 and Equation 13). Consider an anisotropic paper ($A = 2$ in Figure 7) at different total strain. At a given negative total strain the relative decrease in stiffness is larger in MD compared to CD (55% decrease in MD and 35% in CD at –6% total strain). But at the free drying strain in MD and CD respectively the relative

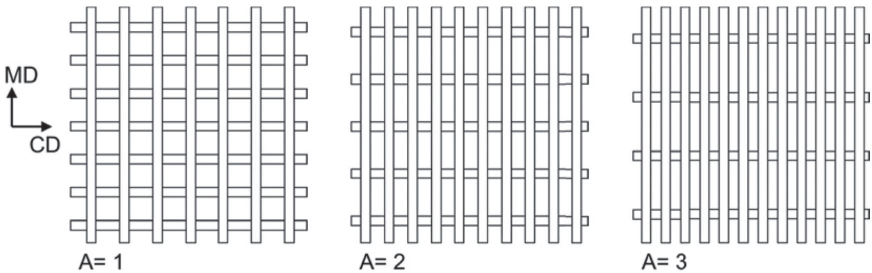

Figure 36. Schematic fibre network with increasing fibre anisotropy, A. The average number of fibres in all in-plane directions are constant which gives the illustrated number of fibres in MD and CD (A = 1: 7 fibres in MD and CD, A = 2: MD 10 and CD 5, A = 3: MD 12 and CD 4).

decrease is larger in CD compared to MD (55% in MD and 70% in CD). The larger relative reduction in CD gives the difference between Equation 12 and Equation 13. The same type of reasoning can be applied for tensile strength, strain at break and tensile energy absorption but the slope of the relations will vary according to the relations proposed in Equation 15, Equation 17 and Equation 19 (based on the experimental results in Figure 25, Figure 27 and Figure 29).

Fibre anisotropy was assumed to be constant with varying total strain in the proposed model. Sometimes it is debated whether a wet draw changes the fibre orientation distribution, and thereby also the fibre anisotropy, by induced fibre rotation. However Danielsen and Steenberg (1947) showed that the fibre anisotropy does not change with increasing MD strain through the machine. Direct measurements on dyed fibres in the paper showed no difference in fibre anisotropy measured at couch, press or reel for a stretch as high as 20% through the machine. Hess and Brodeur (1996) stretched anisotropic hand sheets (Formette) 15 degrees offset to the main axis. The change of the fibre orientation distribution with increased stretch from zero to 2,4% was very small or not significant at all. The lack of influence from a wet stretch on fibre anisotropy is most likely due to bonding, or interlocking of the fibres through other mechanisms, that hinders fibre rotation. If the fibres are anyway assumed to rotate freely the change in fibre anisotropy can be calculated using an analytical solution proposed by Olson et al (2004). R in their Equation 28 can be understood as a flow velocity increase which gives a fibre anisotropy increase of 5% for a 2,4% wet stretch. Since there are a 1:1 relationship between fibre anisotropy and tensile stiffness anisotropy this corresponds to a tensile stiffness increase of 2,5% in MD to be compared with the

20% increase in shown in *Figure 7* for 2,4% stretch and $A(F) = 2$. This means that even if some directional changes of the fibres, or segments between fibre bonds, are possible it is a small effect compared to the direct effect of wet stretch on tensile stiffness through fibre network activation.

The MD strain or press draw between the 2nd press and first dryer group was not accounted for in the predictions of the machine trial. There are also other MD strains in the forming and drying section not accounted for. In practice this means that also the MD strain was used as a tuning parameter. If the known press draw of 2,3 % between 1st and 2nd press had been included the results had been heavily over predicted. The explanation is the linear relation between properties and total strain described by Equation 4. The relationship is not valid for high positive strains where tensile properties are known to reach a maximum or level out (Schulz 1961, Setterholm and Kuenzi 1970). Regarding strains in the dry part of the machine there are very few data available in the literature. Htun (1986) presented results where the effect of a certain MD strain decreases with decreasing moisture content.

Density is assumed to be constant with varying total strain in the proposed model. Basis weight obviously changes proportionally with total strain. Regarding thickness the data is scarce and the situation more unclear in the literature. One reason for this is that with increased shrinkage also comes increased surface roughness which makes the thickness less defined. Wahlström et al (2000) found that the density is constant for different negative total strain (shrinkage), but with increasing positive strain (stretch) from zero to four percent the density decreased around 5 %.

The difference in tensile properties at the edges in the CD direction according to Figure 32 to Figure 35 were obviously due to the MD strain or press draw and the resulting contraction in CD. Wahlström and Fellers (1999, 2000) showed that the total strain accumulated during drying in one principal in-plane material direction of the paper does not have an effect on the relation between tensile properties and total strain in the transversal direction. Note however that when a paper is stretched in one principal material direction it will contract in the transverse in-plane direction. This mechanical deformation will be a part of the total strain accumulated during drying and are assumed to influence the tensile properties according to Equation 4. Strictly the linear relations in Equation 4 has only been shown for different amount of shrinkage and stretch, not contraction in the meaning negative mechanical strain. In lack of dedicated experimental studies the result from the machine trial was studied in detail regarding the contraction in CD and tensile stiffness in CD. Since the two were not measured on equal interval on the CD samples relations were fitted to the experimental data using the proposed model but tuned for best fit according to Figure 37. Thereafter tensile stiffness index in CD was plotted versus total strain in CD (Figure 38). Both the reference

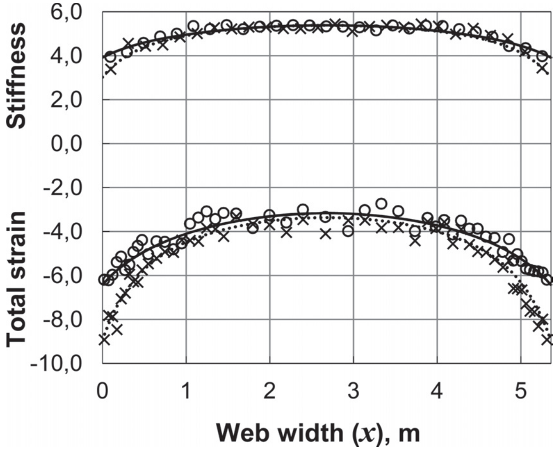

Figure 37. Measured tensile stiffness index (CD) and total strain (CD) versus web width position for the reference case (circles, solid line) and increased draw case (crosses, dotted line).

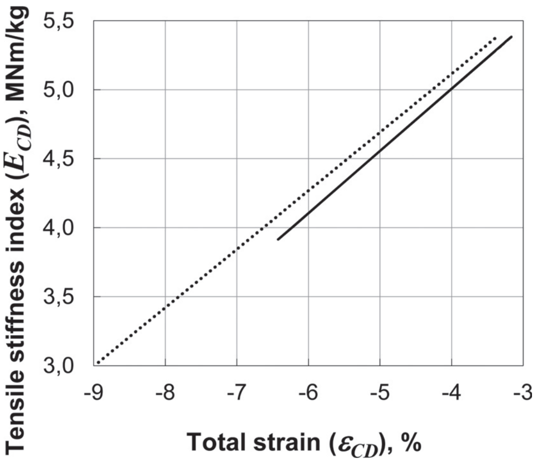

Figure 38. Tensile stiffness index in CD versus total strain in CD for the reference case (solid line) and increased draw case (dotted line).

case and the case with increased MD draw, and thereby also increased CD contraction, showed linear relations. This indicates that a mechanically induced contraction influenced tensile properties according to Equation 4 and also made Equation 26 possible. If another mechanism had been prevailing a deviation from the linear relation would probably have been seen since the two cases were subjected to different amount of contraction or negative mechanical strain. There are indications that a change in press draw also changes the shrinkage behaviour in the following dryer section. This could depend on the increased web tension resulting from the increased press draw. Wahlström (2012) proposed that the main effect from a press draw is caused by the instant CD contraction and this is also the assumption in the proposed model. The final paper width 5,36 m was used both for the reference case and the increased draw case to make the presentation of the results convenient. For the increased draw case the final paper width was 5,22 m which would have influenced the shape of the profile through Equation 25, but only marginally. For the same reason also the same web width was used for both the press and dryer section width (W^p and W^d).

The model contains quite a few parameters, but the great part is measurable on the furnish (Table 1) or on the paper or machine (Table 2). Tuning of the model was limited to the to the three tuning parameters in Table 3 which defines the shape of the total strain profile in CD. It has also been discussed earlier in this work that the MD strain should be seen as a tuning parameter. The use of the parameter "Dryer free draw" for tuning may be motivated from the results by Wahlström et al (1999). They found by simulations that an increasing number of free draws changed the shape of the shrinkage profile. Their results can be predicted using Equation 24 in this work by changing only the "Dryer free draw" parameter. A typical use of this model would be to tune the model further to better fit the experimental data for the reference case. Thereafter the effect of changes in the parameters in Table 2 can be predicted. For the current case the tuning was set to a munimum to illustrate the predictive capacity of the model. The deviation of the predictions from the measurements are given in Table 4. Given the limited tuning of the model the results are fairly good from an engineering point of view. The deviation is around 10% or less for most of the evaluated positions and properties. Exceptions are MD strain at break and MD tensile energy absorption. Predicted MD strain at break was 16% higher compared to measured values for the reference case. Predicted MD tensile energy absorption was as much as 40–50% higher than the measured values. The large deviation originated from the low slope of the relation between TEA anisotropy and tensile stiffness anisotropy in *Figure 29*. For tensile index (Figure 33) the deviations could not be explained by changing the relations between anisotropies. Rather the handsheet data gave too high values compared to the machine data.There are obviously other parameters affecting the tensile properties such as formation, the forming pressing and drying process, differences in sheet structure and retention of the fine material. Still quite a large part of the behaviour can be captured with this model accounting for web width, length of free draws, MD strain, fibre orientation anisotropy and furnish data as input. Therefore the predictive capability of the models is regarded as fairly good, especially since the general behaviour of the tensile property profiles were correctly captured. Combined with the multilayer model proposed by Wahlström and Mäkelä (2005) and Wahlström et al (2008) also changes in a multilayer structure can be predicted.

CONCLUSIONS

The hand sheet trials showed that the geometric mean of tensile stiffness index, tensile index, strain at break, tensile energy absorption and free drying strain in MD and CD was constant and equal to the isotropic value.

Relations between anisotropies of tensile stiffness index, tensile index, strain at break, tensile energy absorption, free drying strain for restrained and free dried papers and fibre anisotropy were established in the handsheet trials.

An engineering model establishing a link between furnish properties and property profiles in MD and CD was proposed for tensile stiffness index, tensile index, strain at break and tensile energy absorption.

Except for MD tensile energy absorption the predictive capability of the model was regarded as fairly good, especially since the general behaviour of the paper properties was correctly captured.

The linear relation between the studied properties and press draw gave too large deviations in predicted properties if the total press draw from forming section to reel was used. The known non-linearity and dependence of moisture content where the draw takes place need to be further studied.

ACKNOWLEDGEMENTS

Stora Enso for supporting this work and Fredrik Nordström, Billerudkorsnäs Gruvön, for the production machine press draw trials.

LITERATURE

Baum, G.A., D.C. Brennan and C.C. Habeger (1981) “Orthotropic elastic constants of paper” Tappi 64(8): 97–101.

Carlsson, L. and C. Fellers (1980) "Flexural stiffness of multi-ply paperboard" Fibre Science and Technology 13: 213–223.

Constantino, P.A., S. I'Anson and W. Sampson (2005) "The effect of machine conditions and furnish properties on paper CD shrinkage profile" The thirteenth Fundamental Research Symposium "Advances in Paper Science and Technology" 11th – 16th September 2005 in Cambridge, UK.

Danielsen, R. and B. Steenberg (1947) "Quantitative determination of fibre orientation in paper" Svensk papperstidning. 50(13): 301.

Hasuike, M., P-Å. Johansson, C. Fellers and O. Terland (1987) "Fiber orientation and its relation to paper formation studied by image analysis" IPPC, Québec, Canada, pp. 185–188.

Hess, T.R. and Brodeur, P.H. (1996). "Effects of wet straining and drying on fibre orientation and elastic stiffness orientation". Journal of Pulp and Paper Science, 22 (5): J160–J164.

Htun, M. (1986) "The control of mechanical properties by drying restraints" in: Paper Structure and Properties (J.A. Bristow and P. Kolseth editors). Marcel Dekker, New York, Basel. Chapter 15, pp. 311– 326.

Htun, M. and C. Fellers. (1982) "The invariant mechanical properties of oriented handsheets". Tappi Journal, 65 (4): 113–117.

I'Anson, S.J., R.P.A. Constantino, S.M. Hoole and W.W. Sampson (2008) "Estimation of the profile of cross- machine shrinkage of paper". Meas. Sci. Technol. 19 (2008).

Mäkelä, P. (2003) "Analysis of the paper web during its passage through the drying section" 2003 International Paper physics Conference, Victoria, British Columbia, September 7–11, 2003, pp.151–155.

Mäkelä (2009) "Effect of drying conditions on the tensile properties of paper" The 14th Fundamental Research Symposium "Advances in Pulp and Paper Research", St Anne's College, 13th – 18th September 2009, Oxford, UK.

Nanko, H. and J. Wu (1995) "Mechanisms of paper shrinkage during drying". International Paper Physics Conference, Niagara-on-the-Lake, Canada, pp. 103–113.

J.A. Olson, I. Frigaard, C. Candice and J.P. Hämäläinen (2004) "Modeling a turbulent fibre suspension flowing in a planar contraction: The one-dimensional headbox" International Journal of Multiphase Flow 30 (2004) 51–66.

de Ruvo, A., R. Lundberg, S. Martin- Löf and C. Söremark (1976) "Influence of temperature and humidity on the elastic and expansional properties of paper and the constituent fibre" (F. Bolam, Ed.) Tech. Div. BPBIF, London 1976, pp. 785.

Rigdahl, M. and H. Hollmark (1986) "Network mechanics" In Paper Structure and Properties (J.A. Bristow and P. Kolseth editors). Marcel Dekker, New York, Basel. Chapter 5, pp. 255–258.

Schrier, B., and H. Verseput (1967) "Evaluating the performance of folding cartons" Tappi 50 (3): 114.

Schulz, J. H. (1961) "The effect of straining during drying on the mechanical and viscoelastic behavior of paper". Tappi Journal, 44 (10): 736– 744.

Setterholm, V.C. and E.W. Kuenzi (1970) "Fiber orientation and degree of restraint during drying. Effect on tensile anisotropy of paper handsheets". Tappi Journal, 53 (10): 1915–1920.

Wahlström, T. (2004) "The invariant shrinkage and stiffness of paper, -modeling anisotropic behavior based on isotropic handsheets" The 2004 progress in paper physics seminar, June 21–24, 2004, NTNU and PFI, Trondheim, Norway.
Wahlström, T. (2009) "Prediction of fibre orientation and stiffness distributions in paper – an engineering approach" The 14th Fundamental Research Symposium "Advances in Pulp and Paper Research", St Anne's College, 13th – 18th September 2009, Oxford, UK.
Wahlström, T. (2012) "Wet stretch of paper and its relation to CD shrinkage and tensile stiffness profiles" International paper physics conference, Stockholm, June 10–14, 2012.
Wahlström, T., K. Adolfsson, S. Östlund and C. Fellers (1999) "Numerical modelling of the cross direction shrinkage profile in a drying section, a first approach" 1999 International Paper Physics Conference, September 26–30, San Diego, CA, pp. 517–531.
Wahlström, T. and C. Fellers. (1999) "Biaxial straining of paper during drying, relations between stresses, strains and properties", TAPPI Engineering Conference, September 12–16, 1999, Anaheim, CA, pp. 705–720.
Wahlström, T. and C. Fellers (2000) "Biaxial straining of handsheets during drying- effect on in-plane mechanical properties" Tappi Journal, 83 (8): 91.
Wahlström, T., C. Fellers and M. Htun (2000) "A laboratory method for biaxial straining of paper during drying". Tappi Journal, 83 (7): 75.
Wahlström, T. and K. Goldzer (2004) "A laboratory method for determining the free shrinkage strain of wet paper" The 2004 progress in paper physics seminar, June 21–24, 2004, NTNU and PFI, Trondheim, Norway, pp. 161–163.
Wahlström, T. and P. Mäkelä (2005) "Predictions of anisotropic multiply board properties based on isotropic ply properties and drying restraints" The 13th FRC "Advances in Paper Science and Technology" 11th – 16th September, Cambridge, UK.
Wahlström, T., A. Lundh, T. Hansson and C. Fellers (2000) "Biaxial straining of handsheets during drying-effect on delamination resistance" Nordic pulp and and paper research journal, 15 (3): 237–242.
Wahlström, T., V. Rakic, H. Karlsson, F. Thuvander and J. Lif (2008) "Predicting tensile properties of multilayer paperboards from properties of the layers" Progress in paper physics seminar, Otaniemi, Espoo, Finland, 2–5 June 2008.

APPENDIX 1

Equation 27 to Equation 42 gives tensile stiffness index, tensile index, strain at break, tensile energy absorption and free drying strain in the MD and CD direction and for free and restrained drying as a function of the respective isotropic property and fibre anisotropy. The equations are derived from and thereby summarises Equation 6 to Equation 20.

$$E^r_{MD} = E^r_{Iso}\sqrt{A(F)} \tag{27}$$

$$E^r_{CD} = E^r_{Iso}\Big/\sqrt{A(F)} \tag{28}$$

$$E_{MD}^{f} = E_{Iso}^{f}\sqrt{2A(F)-1} \tag{29}$$

$$E_{CD}^{f} = E_{Iso}^{f}\Big/\sqrt{2A(F)-1} \tag{30}$$

$$\sigma_{T\,MD}^{\,r} = \sigma_{T\,Iso}^{\,r}\sqrt{A(F)} \tag{31}$$

$$\sigma_{T\,CD}^{\,r} = \sigma_{T\,Iso}^{\,r}\Big/\sqrt{A(F)} \tag{32}$$

$$\sigma_{T\,MD}^{\,f} = \sigma_{T\,Iso}^{\,f}\sqrt{1{,}33A(F)-0{,}33} \tag{33}$$

$$\sigma_{T\,CD}^{\,f} = \sigma_{T\,Iso}^{\,f}\Big/\sqrt{1{,}33A(F)-0{,}33} \tag{34}$$

$$\varepsilon_{T\,MD}^{\,r} = \varepsilon_{T\,Iso}^{\,r} \tag{35}$$

$$\varepsilon_{T\,CD}^{\,r} = \varepsilon_{T\,Iso}^{\,r} \tag{36}$$

$$\varepsilon_{T\,MD}^{\,f} = \varepsilon_{T\,Iso}^{\,f}\Big/\sqrt{0{,}25A(F)+0{,}75} \tag{37}$$

$$\varepsilon_{T\,CD}^{\,f} = \varepsilon_{T\,Iso}^{\,f}\sqrt{0{,}25A(F)+0{,}75} \tag{38}$$

$$W_{MD}^{r} = W_{Iso}^{r}\sqrt{A(F)} \tag{39}$$

$$W_{CD}^{r} = W_{Iso}^{r}\Big/\sqrt{A(F)} \tag{40}$$

$$W_{MD}^{f} = W_{Iso}^{f}\sqrt{0{,}25A(F)+0{,}75} \tag{41}$$

$$W_{CD}^{f} = W_{Iso}^{f}\Big/\sqrt{0{,}25A(F)+0{,}75} \tag{42}$$

$$\varepsilon_{MD}^{f} = \varepsilon_{Iso}^{f}\Big/\sqrt{A(F)} \tag{43}$$

$$\varepsilon_{CD}^{f} = \varepsilon_{Iso}^{f}\sqrt{A(F)} \tag{44}$$

Transcription of Discussion

PREDICTIONS OF MD AND CD TENSILE PROPERTY PROFILES

Torbjörn Wahlström

Stora Enso AB, Box 9090, 650 09 Karlstad, Sweden

Hannes Vomhoff Innventia

At the edges, you have a decrease in the CD tensile stiffness index while the MD tensile stiffness index remains constant. Before, you said that the geometric mean, is always constant; can you apply this also to the edges? What I would have expected is that maybe the MD tensile stiffness index is going up at the edges.

Torbjörn Wahlström

This is a very important part actually. This is only true if the drying conditions are the same.

Additional explanation provided at the end of the discussion for this paper by Torbjörn Wahlström:

That is correct for a special case. The geometric mean is constant with changing fibre orientation anisotropy if the drying restraints are the same in both in-plane directions. However, in a paper machine, the drying restraints are different in MD and CD and one important part of the modelling procedure is how to overcome this. In the presentation, I showed the equations needed to believe in the results. To answer the question we need to be go back to the basis for this model for the link between furnish properties and paper properties. It is the geometric mean, first used by Schrier and Verseput in 1967[1]. They made a machine trial, and it was very varied when they looked at MD and CD properties, but when they applied the

[1]B. Schrier and H. Verseput (1967), "Evaluating the performance of folding cartons", Tappi 50 (3): 114.

geometric mean, suddenly they saw the effect of that trial. My interpretation of this is that they averaged out some variations and fluctuations in fibre orientation. That was a nice finding, and as you all know we use this a lot in the industry just for this reason, also it gives us one number to follow instead of two. In 1982 Htun and Fellers[2] found that the geometric means is equal to the isotopic property but only for constant drying conditions, restrained or free drying. But it was not possible to apply for other combinations, for example a combination of shrinkage and stretch as we have in the position that you were referring to in the question. In 2004 Wahlström[3] found that also the free drying strain follows the behaviour of being equal to the isotopic property and constant with varying fibre orientation. These observations, together with assumed relations between the fibre-, property- and shrinkage anisotropies, enable predictions of the anisotropic material properties for any total strain after drying. Which is exactly what is done in the position that you were referring to.

Hannes Vomhoff

What is different in the drying conditions at the edges? I understand that the deformation of the wet sheet is different at the edges, but what is different regarding the drying conditions at the edges?

Torbjörn Wahlström

As you say it is stretched, then you get the contraction; and it is as simple as that. I cannot see that the drying conditions differ in a way that affects the paper properties.

Hannes Vomhoff

Okay, but the sheet structure at the edges is the same, meaning also the fibre orientation. Do you assume the sheet structure at the edges is the same as in the middle?

[2]M. Htun and C. Fellers. (1982), "The invariant mechanical properties of oriented handsheets", Tappi Journal, 65 (4): 113–117.
[3]T. Wahlström (2004), "The invariant shrinkage and stiffness of paper, – modeling anisotropic behavior based on isotropic handsheets", The 2004 progress in paper physics seminar, June 21–24, 2004, NTNU and PFI, Trondheim, Norway.

Torbjörn Wahlström

Yes, one assumption in this model is that the fibre orientation does not change with shrinkage or stretch and that has been shown by Danielsen and Steenberg (1947)[4] in an old work referred to in the paper. They made experiments on a greaseproof paper machine, inducing stretches as high as 20 percent, and no changes were seen in that work. Actually in the discussion part, I made some simplified calculations, assuming that the fibres are allowed to rotate, how much would that mean to the properties? And even if they are allowed to rotate freely, which of course they are not, then it would be a minor part.

Warren Batchelor Monash University (from the chair)

Is this model able to predict what would happen, for example, if you had a combination of single-tier and two-tier drying where the restraint in each part is quite different?

Torbjörn Wahlström

Yes, absolutely. That is something I use this kind of work for. For example what will happen if we take away a Yankee cylinder? The way of working is simply to split the drying in to smaller parts and do individual simulations. Thereafter the total profile is the sum of the separate parts.

[4]R. Danielsen and B. Steenberg (1947), "Quantitative determination of fibre orientation in paper", Svensk Papperstidning. 50(13): 301.